Minimizing Swing of Suspended Payload of Quadrotor Using Linear Control

Final Report

Bilal Ghader, Kamal Haddad, Samer Abuthaher

Departement Electrical and Computer Engineering

American University of Beirut Beirut, Lebanon

bmg06@mail.aub.edu, kmh16@mail.aub.edu, sma90@mail.aub.edu

***Abstract*— The problem of a quadcopter with a suspended payload is presented, with the purpose of minimizing payload swing using a linear controller. First, the non-linear system is modelled, for the ease of use the model is a 2-dimensional one. After analysis, the system is simulated in MATLAB. Finally, a controller scheme is proposed for solving the problem, and a hovering state feedback controller is presented and assessed.**

Keywords—quadcopters; load; swing effect;

I. INTRODUCTION AND LITTERATURE REVIEW

Recently, quadcopters were treated with increasing interest in the academic field. In the last few years many new applications for quadcopter started to surface, including but not limited to: a possible alternative for human delivery for transporting products that have a relatively a low weight such as the amazon prime air [1] and firefighting application [2]. All these kind of applications raises questions about the interaction between the quadcopters and any possible suspend load that might be attached to it.

In fact, interaction between the load and the air vehicle was raised several times in the field. This issue was studied extensively on the model of the helicopter in the nineties due to its different applications and especially military ones [3][4].

Figure 1: different models of helicopter with suspended load as studied by [4]

With the increasing popularity of vertical take-off and landing vehicles (or VTOL) and specially the quadcopters due to their simple mechanics and ease of control [5] [6]. This interaction between the load and the air vehicle was reconsidered, not only limited to helicopter but also studied on similar system like quadcopters.

To be noted, the work produced in the area is very diverse. For example, some of the work produced was interested in minimizing the effect of the load on the quadcopter [7] during the flight maneuvers, allowing only a minimum amount of disturbance caused by the load. In addition to that some of the work had as goal to minimize the swing of the load. However, it is interesting to notice the different approach to the modeling of this problem.

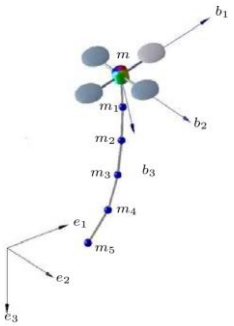

Figure 2: quadcopter with suspended load as modeled by [8]

Figure 2 describes the model used by Goodarzi et al [8] while tackling this problem. The problem models the load of the quadcopter as a serial connection of an arbitrary number of links. However, the main contribution of this work was focused on stabilizing the position of the quadcopter and align the links in a vertical direction after the quadcopter reaches its final destination and not during the flight maneuvers.

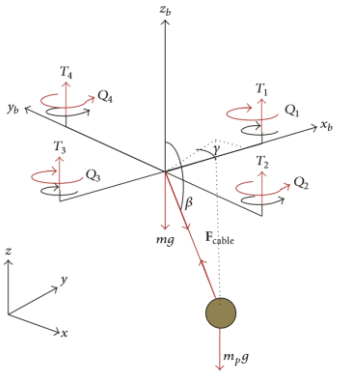

Figure 3: quadcopter with suspended load as considered by [9]

Figure 3 clearly displays that Sadr et al. [9] had a different approach when it comes to modeling the problem. The team considered the cable as one piece, inelastic and with minimal contribution. In addition to that, they considered the inertia matrix to be time invariant and did not take in consideration the effect of the load on the model of the quadcopter. another example can be the work of Koushil et al., [10] focused mainly on a path generation that allowed minimum swing for the load during the trajectory of the quadcopter. The paper also studied different possibilities to exploit the swing of the load to achieve desirable criteria.

The work displayed in this paper, the contribution of the load on the model are taken in consideration. the work will be mostly focused on minimizing the swing of the load. To make, things easier a two dimensional model is considered. The model is assumed to exist only in the $x-y$ plane, reducing the complexity of the system.

After these assumptions, the swing of the load will have only one degree of freedom which is the angle θ. The load is considered to be a point mass, however its contribution to the model is taken in consideration. The link is assumed to be a solid rod with minimal contribution on the model. Model derivation were obtained with the help of the Lagrange's Equations [11] and basic mechanical principles as described in [12]. The Lagrange's equations are based on the principle of energy conservation:

$$L = T - V \tag{1}$$

Where T and V stands for kinetic and potential energy. The Lagrange's equations allow derivation of system dynamics for conservative system by solving the following equation:

$$\frac{d}{dt}\left(\frac{\delta L}{\delta \dot{x}_i}\right) - \frac{\delta L}{\delta x_i} = 0 \tag{2}$$

It is necessary to introduce few terms related to air vehicle engineering. Roll, pitch and yaw are the three axis along which an airplane can rotate. The roll, pitch and yaw angles are also known as the Euler angles and considered as standard in aerospace engineering. Throughout the paper these angles will be designated by the following terms: π for pitch ρ for roll and γ for the yaw. Pitch is the axis running from wing to wing in classical airplane the orientation around the pitch determine whether the airplane is going up or going down. Roll is the front-tail axis of the plane, a change in the roll angle will change the orientation of the wings relatively to each other. and finally the yaw axis, orientation around the yaw axis will change the direction of the plan.

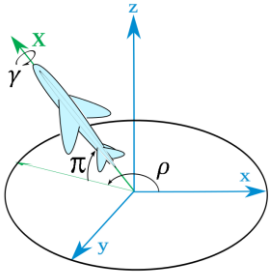

Figure 4: Euler angles on a regular plane [12]

II. Model

Instead of relying on a 3D model of the quad that a derivation of which was attempted in the progress report, a 2D model is obtained instead to simplify manipulation, as shown in figure x. This means that y motion, and roll and yaw rotations, are ignored. For the sake of our problem – as we are interested in static regulation without translational motion along x or y, this model presents a sandbox where the control methods can be tested. For the general case, feedback techniques can be used to project the quad motion into a path to reduce the general motion to this 2D problem, but this will considerably increase the difficulty.

The system model is derived using the Lagrangian, where the terms come as follows

$$L = T - V \tag{1}$$

$$\begin{aligned} T &= KE_q + KE_L \\ &= \frac{1}{2} m_q \left\| \begin{matrix} \dot{x} \\ \dot{z} \end{matrix} \right\|^2 + \frac{1}{2} J_q \dot{\pi}^2 + \frac{1}{2} m_L \left\| \begin{matrix} \dot{x} \\ \dot{z} \end{matrix} \right\|^2 + \frac{1}{2} J_L \dot{\theta} \end{aligned} \tag{3}$$

$$\begin{aligned} V &= PE_q + PE_L \\ &= m_q g z + m_L g (z - L[1 - \cos\theta]) \end{aligned} \tag{4}$$

x, z are the linear coordinates, π being the pitch angle, θ the payload angle, as shown in figure x. m_q and m_L are the masses of the quad and the payload, respectively, while J_q and J_L are the respective moments of inertia around the axis perpendicular to the intersection of the x and z axis shown in the figure. Moreover, L is the length of the payload arm, and g is the acceleration of gravity .

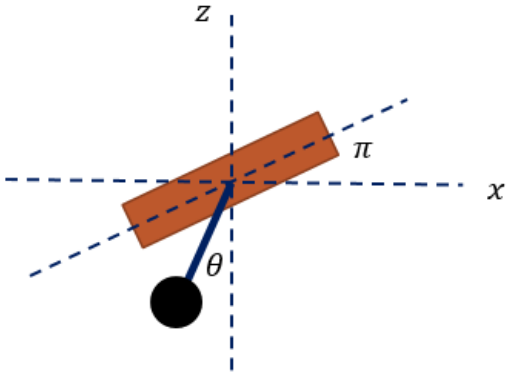

Figure 5: linear and angular conventions, positive angles shown.

Taking the derivatives to derive the equations of motion yields the vectorized Lagrange equation:

$$\frac{\mathrm{d}}{\mathrm{dt}}\left(\overrightarrow{\nabla_{\dot{q}} L}\right) - \overrightarrow{\nabla_q L} = \vec{Q} \tag{5}$$

$$\overrightarrow{\nabla_{\dot{q}} L} = \begin{pmatrix} (m_q + m_L)\dot{x} \\ (m_q + m_L)\dot{z} \\ J_q \dot{\pi} \\ J_L \dot{\theta} \end{pmatrix}$$

$$\frac{\mathrm{d}}{\mathrm{dt}}\overrightarrow{\nabla_{\dot{q}}L} = \begin{pmatrix} (m_q + m_L)\ddot{x} \\ (m_q + m_L)\ddot{z} \\ J_q\ddot{\pi} \\ J_L\ddot{\theta} \end{pmatrix}$$

$$\overrightarrow{\nabla_q L} = \begin{pmatrix} 0 \\ -(m_q + m_L)g \\ 0 \\ Lm_L g\sin\theta \end{pmatrix}$$

$$\vec{Q} = \begin{pmatrix} -F_1\sin\pi \\ F_1\cos\pi \\ F_3 - b(\dot{\pi} + \dot{\theta}) \\ \sin(\theta + \pi)\,F_1 L - b(\dot{\pi} + \dot{\theta}) \end{pmatrix} \quad (6)$$

With b being the viscous friction at the joint securing the hanging mass to the quad. The forces-torques F_1 and F_3 in the quad frame of reference are a transformation of the motor speeds used for convenience. The full transformation as used in other papers [9][] is used, and shown as follows:

$$\overrightarrow{F_q} = \begin{pmatrix} F_1 \\ F_2 \\ F_3 \\ F_4 \end{pmatrix} = \begin{pmatrix} k & k & k & k \\ 0 & -k\cdot L & 0 & k\cdot L \\ k\cdot L & 0 & -k\cdot L & 0 \\ \beta & -\beta & \beta & -\beta \end{pmatrix} \begin{pmatrix} \omega_1^2 \\ \omega_2^2 \\ \omega_3^2 \\ \omega_4^2 \end{pmatrix} \quad (7)$$

In this equation,in ω_i is the angular speed of rotor i, k a coefficient of lift for rotors, β constant times a coefficient of viscous fraction for the rotor blades, and L the distance from the center of each rotor to the center of mass of the quadrotor.

As the matrix multiplying the ω_i^2's is invertible, we can use the forces as control inputs, rather than the angular velocities, and then do the inverse transformation in sending the velocity commands to the motors.

The terms can now be rearranged to a formulation similar to the typical state space formulation as follows:

$$\begin{pmatrix} \ddot{x} \\ \ddot{z} \\ \ddot{\pi} \\ \ddot{\theta} \end{pmatrix} = \begin{pmatrix} 0 \\ -g \\ 0 \\ \dfrac{-g\sin\theta}{L} \end{pmatrix} + \begin{pmatrix} 0 & 0 & 0 & 0 \\ 0 & 0 & 0 & 0 \\ 0 & 0 & -\dfrac{b}{J_\pi} & -\dfrac{b}{J_\pi} \\ 0 & 0 & -\dfrac{b}{J_L} & -\dfrac{b}{J_L} \end{pmatrix} \begin{pmatrix} \dot{x} \\ \dot{z} \\ \dot{\pi} \\ \dot{\theta} \end{pmatrix} + \begin{pmatrix} \dfrac{-\sin\pi}{m_q + m_L} & 0 \\ \dfrac{\cos\pi}{m_q + m_L} & 0 \\ 0 & \dfrac{1}{J_\pi} \\ \dfrac{L\sin(\pi + \theta)}{J_L} & 0 \end{pmatrix} \begin{pmatrix} F_1 \\ F_3 \end{pmatrix} \quad (8)$$

In this equation, the θ, π, x, and z states are omitted for brevity. The system is seen to be causal, lumped, and time-invariant. However, it is not linear, evident in the bias term on $\ddot{z}$, the $\sin\theta$ term on $\ddot{\theta}$, and the non-linear state dependence of the actuator matrix multiplying the force-torques. A compensated force pf the form:

$$F_1 = F_1' + \frac{g(m_L + m_q)}{\cos\pi} \quad (9)$$

includes a bias term that cancels input and bias nonlinearities in $\ddot{z}$. This works especially well when linearizing around $\pi = 0$, which is also another assumption that will be made in linearizing the system.

Linearizing around $\pi = \theta \cong 0$ using small angles approximation, ignoring F_1 effects on θ and π and using compensated F_1 yields

$$\begin{pmatrix} \ddot{x} \\ \ddot{z} \\ \ddot{\pi} \\ \ddot{\theta} \\ \dot{\theta} \end{pmatrix} = \begin{pmatrix} 0 & 0 & 0 & 0 & 0 \\ 0 & 0 & 0 & 0 & 0 \\ 0 & 0 & -\dfrac{b}{J_\pi} & -\dfrac{b}{J_\pi} & 0 \\ 0 & 0 & -\dfrac{b}{J_L} & -\dfrac{b}{J_L} & -\dfrac{g}{L} \\ 0 & 0 & 0 & 1 & 0 \end{pmatrix} \begin{pmatrix} \dot{x} \\ \dot{z} \\ \dot{\pi} \\ \dot{\theta} \\ \theta \end{pmatrix} + \begin{pmatrix} 0 & 0 \\ \dfrac{1}{m_{tot}} & 0 \\ 0 & \dfrac{1}{J_\pi} \\ 0 & 0 \\ 0 & 0 \end{pmatrix} \begin{pmatrix} F_1 \\ F_3 \end{pmatrix} \quad (10)$$

$m_{tot} = m_L + m_q$. Note that only the states that play a role in the dynamics – i.e. ignoring purely integral states – are shown, and the full system needs to include them as a $7x7$ system.

We note that our model neglects atmospheric drag. This will fit our purposes, as we will not be dealing with large velocities for which drag has a significant contribution.

For observability, the paper assumes the quad has perfect sensors capable of measuring all states without error. Thus, the C matrix will be the $7x7$ identity matrix. This makes our system fully state observable.

III. SYSTEM ANALYSIS

We first start by studying the behavior of the payload. As can be seen from the system equations, the payload acts as a simple accelerating pendulum, which is described by the characteristic ODE:

$$J_L\ddot{\theta} + b\dot{\theta} + mgL\sin\theta = (\cos\theta \quad -\sin\theta)\begin{pmatrix} \ddot{x} \\ \ddot{z} \end{pmatrix} \quad (11)$$

In studying the behavior of the suspended payload, two phase portraits were obtained; in presence and the absence of input forces, or accelerations, on our system:

A. no input forces were applied

After performing a phase plane analysis of θ and $\dot{\theta}$,the following figure was obtained:

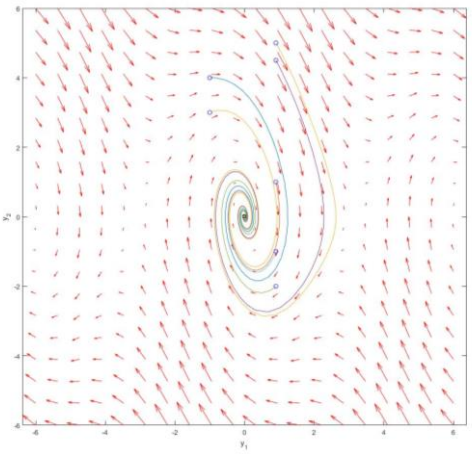

Figure 6: Phase plan analysis of theta vs theta dot with zero input force.

At any point in the plane, the system is driven to a stable point which is the equilibrium point (0;0). Spiral shaped trajectories are displayed. The system exhibits a stable focus node, that repeats every $2\pi n$ with n an integer – typical of angular quantities. This phase portrait shows that, for almost any initial conditions the pendulum would eventually fall back to its rest position. This is expected, as the model of interaction between the two states is exactly the same as the model of a stationary pendulum; without a real impact from the rest of the quad.

B. acceleration applied on the x axis

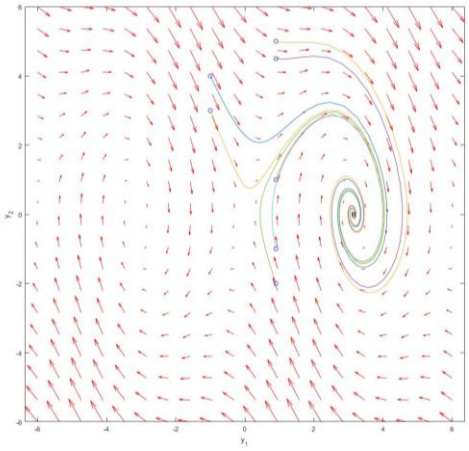

Figure 7: Phase plan analysis of theta vs theta dot with input force taken into account.

The second phase plan analysis takes in consideration the contribution of input acceleration. This has the effect of shifting the equilibrium position of the pendulum; replotting the phase plan analysis, the system maintains its propriety of stable focus but, the location of the stable node is changed. This shows from the ODE of the system, as an acceleration shows as a forcing term, adding a bias term to solutions of the equation. Physically, it shows in that, the old equilibrium point loses its status as the fictitious force pushes the payload away from the direction of the acceleration. Solving for the new equilibrium point yields

$$\theta_{eq} = \arctan\frac{\ddot{x}}{mgL + \ddot{z}} \tag{12}$$

While interactions of the pendulum alone, or the states alone, are relatively simple, the interactions between the different states are a bit harder to describe using phase portraits due to involving more than 3 states. The non-linearities in the system, and input coupling, make the system a bit complicated to predict and analyze. However, since the purpose of this paper is not targeted towards any complicated maneuvers; rather, the system is linearized about a stationary hovering point, the system can be decomposed into 2 independent parts.

The first part is the hovering system, described by the equations:

$$\begin{pmatrix}\ddot{z}\\ \dot{z}\end{pmatrix} = \begin{pmatrix}0 & 0\\ 1 & 0\end{pmatrix}\begin{pmatrix}\dot{z}\\ z\end{pmatrix} + \begin{pmatrix}1\\ 0\end{pmatrix}F_1{}' \tag{13}$$

The system is fully controllable, as can be seen from the controllability matrix:

$$ctrb(A,B) = \begin{pmatrix}1 & 0\\ 0 & 1\end{pmatrix} \tag{14}$$

Which is full-rank, so the system is fully controllable. The second part is the angular quantities system described by:

$$\begin{pmatrix}\ddot{\pi}\\ \ddot{\theta}\\ \dot{\pi}\\ \dot{\theta}\end{pmatrix} = \begin{pmatrix}-\frac{b}{J_\pi} & -\frac{b}{J_\pi} & 0 & 0\\ -\frac{b}{J_L} & -\frac{b}{J_L} & 0 & -\frac{g}{L}\\ 1 & 0 & 0 & 0\\ 0 & 1 & 0 & 0\end{pmatrix}\begin{pmatrix}\dot{\pi}\\ \dot{\theta}\\ \pi\\ \theta\end{pmatrix} + \begin{pmatrix}\frac{1}{J_\pi}\\ 0\\ 0\\ 0\end{pmatrix}F_3 \tag{15}$$

Using MATLAB, the system is found to be full rank, and thus fully controllable as well.

We note that our equations marginalized out the x, as the direct linearized system does not show it; a change in pitch angle is necessary to actuate x. For the purpose of this paper, we are not interested in movement along x, so it is not included in the controller – Controllers that deal with better with nonlinearities might be more suitable for this purpose.

IV. Controller Design and Simulation

A controller design considered is based on a full-state feedback controller, where K_z controls the position in the z-direction of the quadrotor, K_π controls the pitch angle of the quadcopter, and K_Θ controls the angle of the load with respect to the y-axis. Two controllers are needed in this case, one for the z position and another for π, and Θ, as the two are controlled by a single actuating signal.

The output of the controller is then mapped into another controllable form actuating directly the angular speeds of the 4 motors of the quadrotor.

In practice, the states will be measured then fed-back into a low pass filter to remove the high frequency noise resulting from the sensors (accelerometer, gyroscope), knowing that the controller efficiency will be deteriorated. However, for the purposes of this paper, sensors are assumed to be perfect and thus there would not be a low-pass filter on the feedback path.

The block diagram below summarizes how the controller will be implemented.

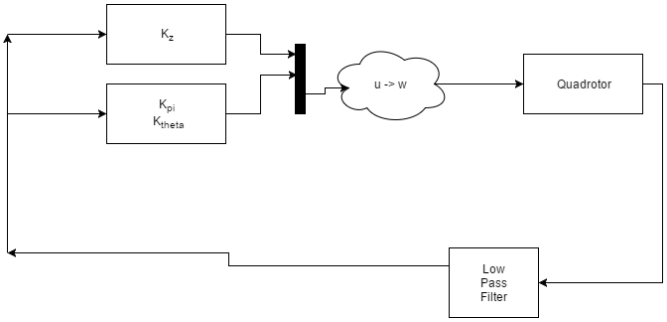

Figure 8: Block diagram of the State Feedback controller

The state feedback controller was done using feedback from the z position, the pitch π, and the angle Θ. For the z-position controller, a basic pole placement regulator was designed by choosing $\omega_n = 8 rad/s$ and $\xi = 0.6$, then the closed loop poles are -4.8 +6.4i, and -4.8 – 6.4i. As for the π and Θ, the same poles were chosen with an additional 2 poles at -10 and -14. Simulations of the model were done with $z = -0.2m, \pi = 0.4rad, and\ \Theta = 0.3rad$ as initial conditions. The z-response, and the π and Θ responses of the controlled model, respectively, are shown in the two figures below.

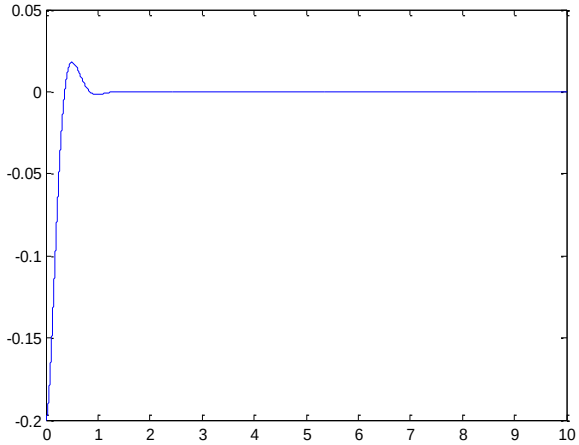

Figure 9: z-response of state feedback controlled system

The z-response of the state feecback controlled system shows an overshoot of 1.8%, a steady state error of 10^{-10}m, a rise time of 0.368s, and a settling time of 1.32s.

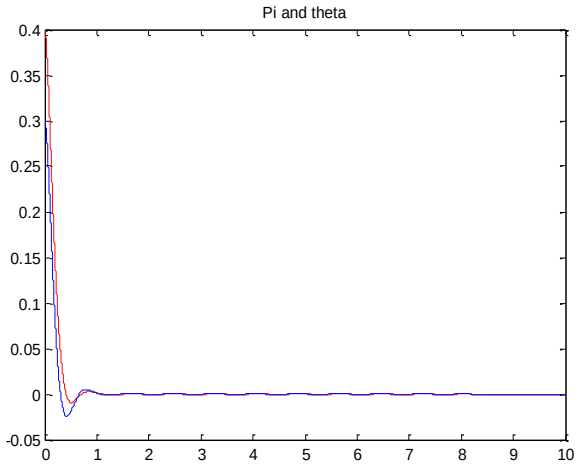

Figure 10: π, Θ responses of state feedback-controlled system

As for the π response, it has a 0.9% overshoot, a steady state error of almost 0, a rise time of 0.4s, and a settling time of 1.4s. The Θ response indicates an overshoot of 2.38%, a steady state error of almost 0, a rise time of 0.31s, and a settling time of 1.3s.

Two LQR controllers were also used on the system, again one for the z-position, and another for the Θ and π. Q was tuned to $\begin{pmatrix} 200 & 0 \\ 0 & 1000 \end{pmatrix}$ and $R = 1$, for the z-position controller. The 2nd controller was tuned to $Q = \begin{pmatrix} 1 & 0 & 0 & 0 \\ 0 & 250 & 0 & 0 \\ 0 & 0 & 300 & 0 \\ 0 & 0 & 0 & 100 \end{pmatrix}$ and R=1. The z, π, and Θ responses are shown in the figures below with the same initial conditions as the simulations done before.

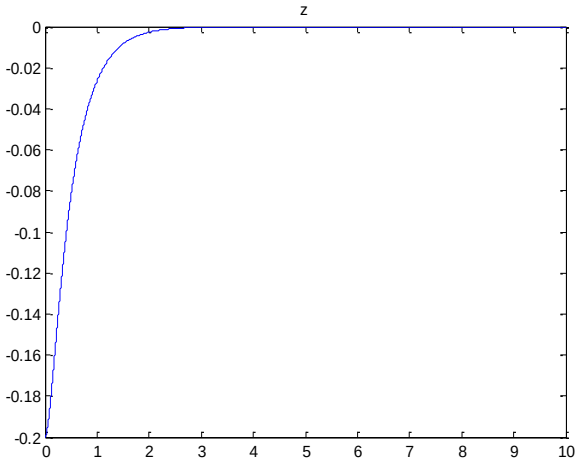

Figure 11: z-response of LQR-controlled system

The z-response of the LQR-controlled system shows no overshoot, a steady state error of approximately 0, a rise time of 2.3s, and a settling time of 2.6s.

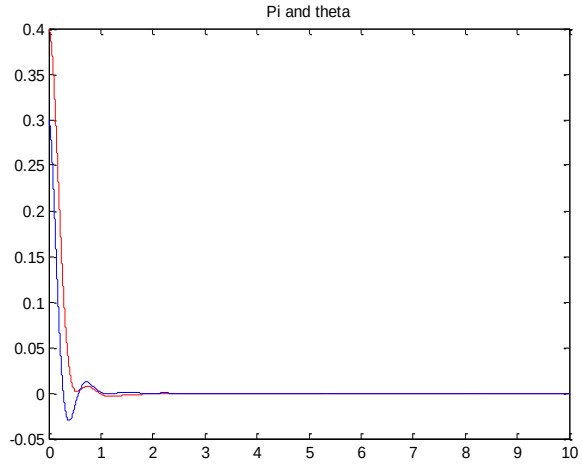

Figure 12: π, θ responses of LQR-controlled system

The π response indicates a 0.3% overshoot, a steady state error of almost 0, a rise time of 1.04s, and a settling time of 2.5s. As for the θ response, it shows an overshoot of 3% with a steady state error of almost 0, a rise time of 0.28s, and a settling time of 1.9s.

These results show that the state feedback controller has a faster response in terms of rise time and settling time for z, π, and θ. Additionally, the linearized state feedback controller shows a higher overshoot for these states than the LQR controller. The LQR gains can be further tweaked to obtain different responses, depending on desired specifications.

Both controllers give approximately 0 steady state error for all states, as well.

The difference between the LQR and the pole placement filters is seen in the control signals – the designed LQR, being slower, gave less control effort than the pole placement controller. Figures 17 and 18 show the control signals for both controllers designed, when regulating the z axis. The lower control signal for the LQR controller is expected, as it tries to optimize partially with respect to a lower control signal.

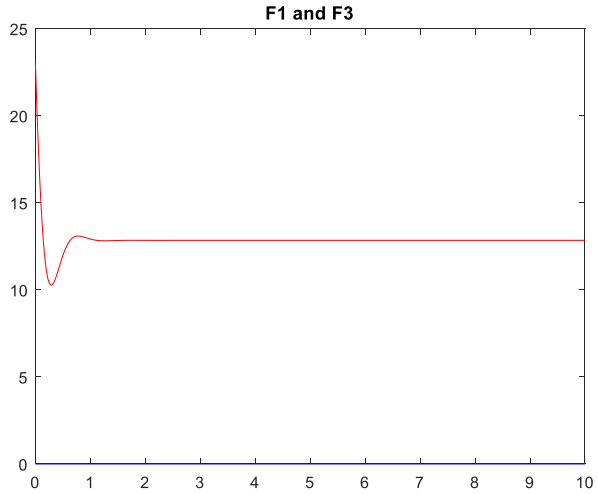

Figure 13: Control signal for z-regulation pole placement controller

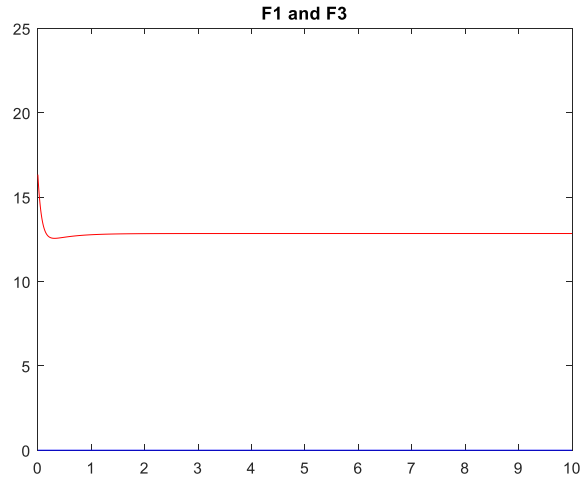

Figure 14: Control signal for z-regulation LQR

Taking a Gaussian-distributed disturbance on $\ddot{z}$, with mean 0 and variance 0.01, to simulate real life conditions, yields the response in figure 19.

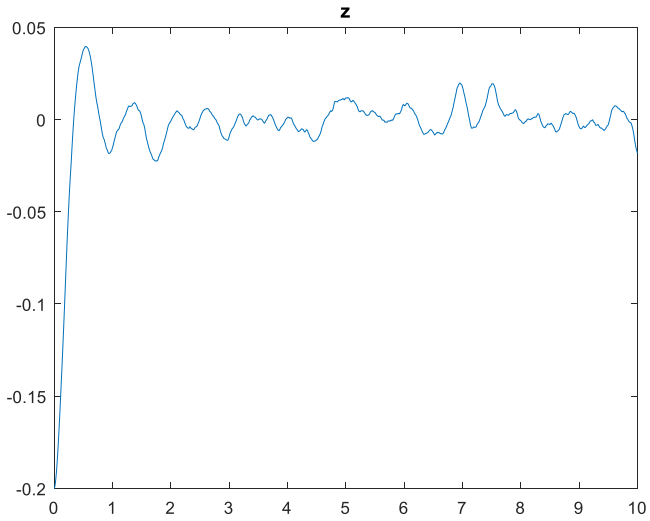

Figure 15: z response of system with Gaussian disturbance

The figure shows the controller regulating the z response even in presence of the noise. Upon settling, the quad would start to fidget around the settling point because of the disturbance. However, those oscillations are less than 2cm, or 10% in magnitude. An approach that would reject those oscillations would be an appropriate disturbance observer and a fast-enough controller.

As a supplement to the designed controller, a disturbance observer for the z subsystem is considered. The subsystem with the disturbance is modelled as:

$$\begin{pmatrix} \ddot{z} \\ \dot{z} \\ \dot{d} \end{pmatrix} = \begin{pmatrix} 0 & 0 & 1 \\ 1 & 0 & 0 \\ 0 & 0 & 0 \end{pmatrix} \begin{pmatrix} \dot{z} \\ z \\ d \end{pmatrix} \quad (16)$$

As for the output equation, the observer will depend only on the measurement of z:

$$y = (0\ 1\ 0) \begin{pmatrix} \dot{z} \\ z \\ d \end{pmatrix} \quad (17)$$

This subsystem would give us the following observability matrix: $\omega_O = \begin{pmatrix} 0 & 1 & 0 \\ 1 & 0 & 0 \\ 0 & 0 & 1 \end{pmatrix}$

Since $rank(\omega_O) = 3$, the subsystem under investigation is completely state observable. The open-loop transfer function is the following: $\begin{vmatrix} s & s & s-1 \\ s-1 & s & s \\ s & s & s \end{vmatrix} = s.$

By identification, in the equation:

$a_2 * s^2 + a_1 * s + a_0,\ a_2 = 0\ ; a_1 = 1\ ; a_0 = 0\ .$

The transformation matrix would be the following,

$$T_{so} = \omega_O^{-1}(A, C) \begin{pmatrix} 1 & 0 & 1 \\ 0 & 1 & 0 \\ 1 & 0 & 0 \end{pmatrix}^{-1} = \begin{pmatrix} 0 & 1 & 0 \\ 0 & 0 & 1 \\ 1 & 0 & -1 \end{pmatrix}$$

Placing three poles at -15, our $CLCE = (s+15)^3 = s^3 + 45s^2 + 675s + 3375.$

$J_\theta = \begin{bmatrix} 3375 \\ 674 \\ 45 \end{bmatrix}.$

$J = T_{SO} * J_\theta = \begin{bmatrix} 674 \\ 45 \\ 3330 \end{bmatrix}.$

The final transfer function is thus the following:

$$\hat{\dot{X}} = A * \hat{X} + Bu + J(y - C * \hat{X})$$

The disturbance d can now be used in the controller, instead of using a hard-coded bias term. This works well with the assumption that d is a step, as it's similar to the $-g$ term. Functionally, controlling based on the observer is similar to adding an I term in a PID controller, which would eliminate steady state errors.

In the mathematical system presented here, disturbance did not have a large impact, so it was not incorporated in the controllers. However, it is expected that a real life system will be more affected by this, so a disturbance observer would lead to a better performance.

V. PRACTICAL CONSIDERATION

All work done in this report assumes perfect sensors on all states. However, this is not the case in reality; sensors are generally noisy and inaccurate in some instances, so care must be taken to choose the correct sensors.

For measuring the angular orientation; the pitch, roll, and yaw angles, an accelerometer combined with a gyroscope can be used.

The accelerometer detects the acceleration vector acting on the quad, and since the quad operates under the effect of gravity, this can be turned to an orientation in space. By nature, however, an accelerometer gives noisy readings. This is where the gyroscope comes in; the gyro measures the angular speeds, which can be integrated to give angular positions that are accurate on the short term. However, integrating the signal is prone to drift, which would yield to long-term underestimation of the position.

To get around that, a complimentary filter can be utilized; giving larger weight on the gyroscope to get accurate short-term estimates, and lower on the accelerometer to correct for the drift on the long term. One implementation of this is shown in [x]. A Kalman filter can also be used, further incorporating the system dynamics for a more precise estimate.

For measuring the z position, an ultrasonic sensor can be used, however the measurements have a Gaussian error. A simple recursive state estimator or a Kalman filter can be used to obtain more accurate measurements. The z velocity can be estimated by taking the derivative of the z position.

For measuring the linear velocities, one approach would be to integrate the accelerometer readings after removing gravity. However, in practice this is difficult to do, mainly because of the noise of the accelerometer. Using an external position feedback system, like vision based systems, is possible, but an integrated solution within the quad is preferred. More research should be done into this.

For measuring the angular position and velocity of the payload, an encoder can be placed on the joint, or an IMU can be placed at the end of the payload arm.

More work will be done to evaluate the effectiveness of those sensor configurations.

VI. CONCLUSION

In this paper, the problem of a 2-dimensional quadcopter with a suspended payload is presented. First, a model is obtained of the system through force equations, and some analysis of the non-linear model is presented, and some simulation is shown. After linearizing, the system is shown to decouple into two subsystems for stable hover conditions; one for the linear motion and one for angular.

A control scheme is developed, in terms of two controllers each operating on a different subsystem. Pole placement and LQR techniques were followed, and the results and simulations were discussed. Some interesting part can be done in researching the instrumentation part of the project, and the paper presented some possibilities for sensor configurations.

The system can be extended to track a path while minimizing swing. To do that, more work should be done in generalizing the system into 3 dimensions. An approach where a trajectory is generated, then the system linearized around a 2-dimensional plane along the direction of motion should give similar results, but more research is necessary. Furthermore, incorporating the disturbance observer in the system would likely yield better real world performance. Finally, some other problems, such as having an actuated link, or a flexible linking arm, would be interesting augmentation to the problem at hand.

VII. NOMENCLATURE

ρ	Roll angle / axis
π	Pitch angle / axis
γ	Yaw angle /axis
ω_i	Angular speed of the motor i
L	Lagrangian
T	Kinetic energy associated with the Lagrangian
V	Potential energy associated with the Lagrangian
Q	Generalized constraint force
PE_q	Potential energy of the quad
PE_L	Potential energy of the load
KE_q	Kinetic Energy of the quad
KE_L	Kinetic energy of the load
m_q	mass of the quad
g	Acceleration of the gravity
m_l	Mass of the load
J_π	Moment of inertia along the pitch angle
J_L	Moment of inertia of the load along joint
b	Coefficient of viscous friction of the joint
θ	Angle between the inertial $\hat{y}_i$ axis and the payload arm.
ω_n	Natural frequency of the system
p_i	Pole placed using pole placement technique

VIII. REFERENCES

[1] "Amazon drone trial gets US regulator approval - BBC News", BBC News, 2015. [Online]. Available: http://www.bbc.com/news/business-31975464

[2] M. Huber, "Unmanned K-Max Tested for Firefighting", Aviation International News, 2014. [Online]. Available: http://www.ainonline.com/aviation-news/business-aviation/2014-12-11/unmanned-k-max-tested-firefighting

[3] R. Stuckey, *Mathematical modelling of helicopter slung-load systems*. Fishermans Bend, Vic.: Aeronautical and Maritime Research Laboratory, 2001, pp. 6-11 and 48-52.

[4] A. McCoy, "Flight testing and real-time system identification analysis of a UH-60A Black Hawk Helicopter with an instrumented external sling load", Master, Monterey, California. Naval Postgraduate Schoo, 2016.

[5] S. Bouabdallah, "Design and Control of Quadrotors With Application to Autonomous Flying", PhD, École polytechnique fédérale de Lausanne, 2007.

[6] G. Hoffman, H. Huang, S. Waslander and C. Tomlin, "Quadrotor helicopter flight dynamics and control: Theory and experiment", in Proc. of the AIAA Guidance, Navigation, and Control Conference,

[7] Pizetta, A. Brandão and M. Sarcinelli-Filho, "Modelling and Control of a Quadrotor Carrying a Suspended Load", in *Workshop on Research, Education and Development of Unmanned Aerial Systems (RED-UAS)*, Cancun, Mexico, 2016.

[8] F. Goodarzi, D. Lee and T. Lee, "Geometric control of a quadrotor UAV transporting a payload connected via flexible cable", *International Journal of Control, Automation and Systems*, vol. 13, no. 6, pp. 1486-1498, 2015.

[9] S. Sadr, S. Moosavian and P. Zarafshan, "Dynamics Modeling and Control of a Quadrotor with Swing Load", *Journal of robitcs*, vol. 2014, 2016.

[10] K. Sreenath, N. Michael and V. Kumar, "Trajectory Generation and Control of a Quadrotor with a Cable-Suspended Load – A Differentially-Flat Hybrid System", in *International Conference on Robotics and Automation (ICRA)*, Karlshue, Germany, 2013, pp. 4888-4895.

[11] John Deyst, and Jonathan How. *16.61 Aerospace Dynamics.* Spring 2003. Massachusetts Institute of Technology: MIT OpenCourseWare, https://ocw.mit.edu

[12] D. Morin, *Introduction to classical mechanics*. Cambridge, UK: Cambridge University Press, 2008.

[13] "Euler angles", *En.wikipedia.org*, 2016. [Online]. Available: https://en.wikipedia.org/wiki/Euler_angles. [Accessed: 06- Nov- 2016].